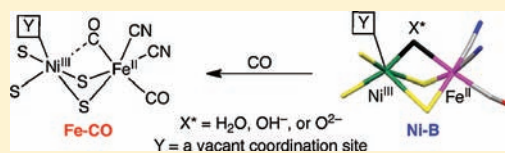


## Model Study of CO Inhibition of [NiFe]hydrogenase

Takahiro Matsumoto,<sup>†,‡</sup> Ryota Kabe,<sup>†</sup> Kyoshiro Nonaka,<sup>†,‡</sup> Tatsuya Ando,<sup>†</sup> Ki-Seok Yoon,<sup>†,§</sup> Hidetaka Nakai,<sup>†,‡</sup> and Seiji Ogo<sup>\*,†,‡,§</sup><sup>†</sup>Department of Chemistry and Biochemistry, Graduate School of Engineering, Kyushu University, 744 Moto-oka, Nishi-ku, Fukuoka 819-0395, Japan<sup>‡</sup>International Institute for Carbon-Neutral Energy Research (I<sup>2</sup>CNER), 744 Moto-oka, Nishi-ku, Fukuoka 819-0395, Japan<sup>§</sup>Core Research for Evolutional Science and Technology (CREST), Japan Science and Technology Agency (JST), Kawaguchi Center Building, 4-1-8 Honcho, Kawaguchi-shi, Saitama 332-0012, Japan

Supporting Information

**ABSTRACT:** We propose a modified mechanism for the inhibition of [NiFe]hydrogenase ([NiFe]H<sub>2</sub>ase) by CO. We present a model study, using a NiRu H<sub>2</sub>ase mimic, that demonstrates that (i) CO completely inhibits the catalytic cycle of the model compound, (ii) CO prefers to coordinate to the Ru<sup>II</sup> center rather than taking an axial position on the Ni<sup>II</sup> center, and (iii) CO is unable to displace a hydrido ligand from the NiRu center. We combine these studies with a reevaluation of previous studies to propose that, under normal circumstances, CO inhibits [NiFe]H<sub>2</sub>ase by complexing to the Fe<sup>II</sup> center.



## INTRODUCTION

Recently, much attention has focused on developing an understanding of the class of enzymes known as hydrogenase (H<sub>2</sub>ase, Figure 1) since it can extract electrons from H<sub>2</sub>.<sup>1–5</sup> Such studies could lead to major developments in clean, green power cell technologies if successfully transferred to industrial processes.<sup>6</sup>

In order to advance the understanding of H<sub>2</sub>ase, we reported the synthesis, structure, and mode of action of a chemically simple [NiFe]H<sub>2</sub>ase mimic.<sup>7</sup> This mimic is based around a NiRu core, and we have been able to fully replicate the three chemically significant functions of H<sub>2</sub>ase, that is, heterolytic activation of H<sub>2</sub>, electron transfer from the H<sub>2</sub>ase mimic to another molecule, and simultaneous isotope exchange between H<sub>2</sub> and D<sub>2</sub>O.<sup>8–11</sup>

Following this progress in understanding H<sub>2</sub>ase activity, we turned to studies of the inhibitory effect of CO on [NiFe]H<sub>2</sub>ase. It is known that CO effectively inhibits H<sub>2</sub>ase, and this behavior has been studied in a number of in vitro investigations using samples of [NiFe]H<sub>2</sub>ase.<sup>1,3c,12</sup>

These studies suggest that CO coordinates to the Ni center, leaving a vacant site between the Ni and the Fe centers. This proposal is based on an interesting crystal structure of the CO-complexed enzyme, Ni–SCO, produced by Higuchi and co-workers (Figure 2),<sup>3c</sup> as well as supporting experimental and theoretical data, provided by Lubitz and co-workers.<sup>1g,12c</sup>

We note that the crystal structure of the CO complex (Ni–SCO) is closer to that of the hydride complex (Ni–C) than the resting complex (Ni–B). Specifically, in the Ni–SCO crystal structure, the Ni···Fe distance (2.61 Å) and Ni–S–Fe bite angles (69.7° and 70.1°) are similar to those of the hydrido-coordinated Ni–C state (2.55 Å; 65.8° and 68.6°, respectively). In other words, it is highly likely that the proposed CO complex

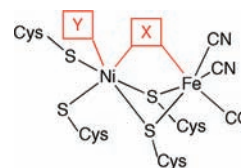


**Figure 1.** Active site structure of [NiFe]H<sub>2</sub>ase. X and Y: possible coordination sites of H<sub>2</sub>O, OH<sup>−</sup>, O<sub>2</sub><sup>2−</sup>, OOH<sup>−</sup>, H<sup>+</sup>, and CO.

bears a bridging hydrido ligand between the metal centers rather than a vacant site.

Furthermore, coordination of the CO to the Ni<sup>II</sup> site rather than Fe<sup>II</sup> is a little perplexing in the context of two vacant sites (X and Y). It is a well-known principle that a  $\pi$ -acceptor ligand, such as CO, would prefer to bind to a low-spin Fe<sup>II</sup> or Ru<sup>II</sup> ion rather than a Ni<sup>II</sup> ion if given the choice. This reasoning leads us to suggest that the Fe<sup>II</sup> site is already occupied, presumably by a hydrido ligand (Ni–HCO, Figure 2).

Although the crystallographic studies of [NiFe]H<sub>2</sub>ase are important, it should be noted that they deviate somewhat from the natural behavior of H<sub>2</sub>ase. For instance, H<sub>2</sub>ase is notoriously sensitive to oxidation, which severely complicates in vitro studies of the native enzyme.<sup>1–5</sup> In fact, these [NiFe]H<sub>2</sub>ase crystal structures have necessarily been produced from samples of [NiFe]H<sub>2</sub>ase that are oxidized with respect to the natural state (Figure 2). For example, the apparent resting state, Ni–B, is actually at the +1 state, relative to natural [NiFe]H<sub>2</sub>ase, and the apparent reduced state, Ni–C, is only −1, as opposed to −2.<sup>1–5</sup>

Received: May 9, 2011

Published: August 19, 2011

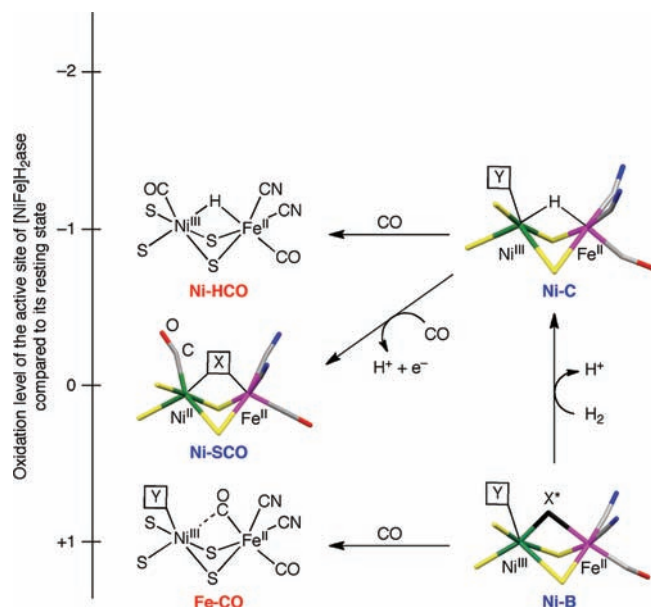


**Figure 2.** CO inhibition of  $[\text{NiFe}]_{\text{H}_2\text{ase}}$ . The structures of Ni–SCO,<sup>3c</sup> Ni–C,<sup>3b</sup> and Ni–B<sup>2,3d,3e</sup> were determined by X-ray analysis. Ni–HCO and Fe–CO are proposed in this paper. X and Y: vacant coordination sites. X\*:  $\text{H}_2\text{O}$ ,  $\text{OH}^-$ , or  $\text{O}^{2-}$ .

With regard to the experimental study of such active sites, the techniques of bioinspired catalysis lend a number of distinct advantages that more than compensate for the inherent shortcomings of a model study.<sup>13</sup> Our  $[\text{NiFe}]_{\text{H}_2\text{ase}}$  mimic is chemically simple and therefore relatively easy to synthesize, handle, and analyze. Furthermore, continuous handling of compounds in reduced states is a common technique in organometallic chemistry. It is therefore relatively straightforward to conduct a range of tests while keeping our model compound away from the corrupting influence of  $\text{O}_2$ . While these advantages have to be taken with the caveats that (i) CO binds more strongly to  $\text{Ru}^{\text{II}}$  than to  $\text{Fe}^{\text{II}}$  and (ii) enzyme active sites have a complex range of interactions with neighboring residues that are not present in our simple model, we believe that the strong correlation between the chemical behavior of our model compound with that of natural  $[\text{NiFe}]_{\text{H}_2\text{ase}}$  is significant evidence that our compound is an effective mimic. We feel, therefore, that conclusions drawn from this study should carry much weight in the assessment of evidence regarding the true action of  $[\text{NiFe}]_{\text{H}_2\text{ase}}$ .

With these considerations in mind, we have been able to conduct a study of the influence of CO on our  $[\text{NiFe}]_{\text{H}_2\text{ase}}$  mimic at oxidation levels which are identical to that found in the native enzyme. As expected, we demonstrate an effective inhibition of  $\text{H}_2$  activation by CO, analogous to that seen in the natural  $[\text{NiFe}]_{\text{H}_2\text{ase}}$ . We use these results to propose a revised model for CO inhibition of  $\text{H}_2\text{ase}$  and thereby place more pieces of the puzzle presented by these tantalizing enzymes.

## EXPERIMENTAL SECTION

**Materials and Methods.** All experiments were carried out under an  $\text{N}_2$  or Ar atmosphere using standard Schlenk techniques and a glovebox.  $[\text{Ni}^{\text{II}}\text{LRu}^{\text{II}}(\text{OH}_2)(\eta^6\text{-C}_6\text{Me}_6)](\text{NO}_3)_2$  **[1]** ( $[\text{1}](\text{NO}_3)_2$ , L = *N,N'*-dimethyl-*N,N'*-bis(2-mercaptoethyl)-1,3-propanediamine},  $[\text{Ni}^{\text{II}}\text{LRu}^{\text{II}}(\text{OH}_2)(\eta^6\text{-C}_6\text{Me}_6)](\text{OTf})_2$  **[1]** ( $[\text{1}](\text{OTf})_2$ , OTf =  $\text{CF}_3\text{SO}_3^-$ ), and  $[\text{Ni}^{\text{II}}(\text{OH}_2)\text{L}(\mu\text{-H})\text{Ru}^{\text{II}}(\eta^6\text{-C}_6\text{Me}_6)](\text{NO}_3)_2$  **[2]** ( $[\text{2}](\text{NO}_3)_2$ ) were

prepared by the methods described in the literature.<sup>7</sup> The manipulations in acidic media were carried out with plastic and glass apparatus (without metal components). Distilled  $\text{H}_2\text{O}$ , 0.1 M NaOH/ $\text{H}_2\text{O}$ , and 0.1 M  $\text{HNO}_3/\text{H}_2\text{O}$  were purchased from Wako Pure Chemical Industries, Ltd.,  $\text{D}_2\text{O}$  (99.9% D) and  $^{13}\text{C}$  (99%  $^{13}\text{C}$ ) were purchased from Cambridge Isotope Laboratories, Inc.,  $\text{H}_2$  (>99.9999%) was purchased from Taiyo Toyo Sanso Co., Ltd., and CO (>95%) was purchased from Sumitomo Seika Chemicals Co., Ltd.

$^1\text{H}$  NMR and  $^{13}\text{C}$  NMR spectra were recorded on a JEOL JNM-AL300 spectrometer. The  $^1\text{H}$  chemical shifts were referenced to 3-(trimethylsilyl)propionic-2,2,3,3- $d_4$  acid sodium salt (TSP, 0.00 ppm), and  $^{13}\text{C}$  chemical shifts were referenced to 1,4-dioxane (67.40 ppm). Electrospray ionization mass spectrometry (ESI-MS) data were obtained by an API 365 triple-quadrupole mass spectrometer (PE-Sciex) and a JEOL JMS-T100LC. IR spectra were recorded on a Thermo Nicolet NEXUS 870 FT-IR instrument using  $2\text{ cm}^{-1}$  standard resolution at ambient temperature. UV–vis spectra were recorded on a JASCO V-670 UV-visible-NIR Spectrophotometer (light path length 1.00 cm) and an Otsuka Electronics photodiode array spectrometer MCPD-2000 with an Otsuka Electronics optical fiber attachment (light path length 1.09 cm). An X-ray photoelectron spectrum (XPS) was measured on a VG Scientific ESCALAB MK II electron spectrometer by use of Mg K $\alpha$  radiation, and the binding energies were corrected by assuming the C 1s binding energy of the carbon atoms of the ligand in specimens as 284.5 eV.<sup>14</sup> In a pH range of 4.0–9.0, the pH values of the solutions were determined by a pH meter (model TOA HM25G) equipped with a pH combination electrode (model TOA GST-5725C) and a pH meter (model IQ Scientific Instruments, Inc. IQ200) equipped with a stainless steel-micro pH probe (model IQ Scientific Instruments, Inc. PH15-SS). Values of pD were corrected by adding 0.4 to the observed values (pD = pH meter reading + 0.4).<sup>15</sup>

$[\text{Ni}^{\text{II}}\text{LRu}^{\text{II}}(\text{CO})(\eta^6\text{-C}_6\text{Me}_6)](\text{NO}_3)_2$  **[3]** ( $[\text{3}](\text{NO}_3)_2$ ). An aqueous solution (5.0 mL) of **[1]** ( $[\text{1}](\text{NO}_3)_2$ ) (328 mg, 0.48 mmol) was purged with CO for 1 h at 25 °C. The solvent of the resulting solution was removed under reduced pressure to yield a brown powder of **[3]** ( $[\text{3}](\text{NO}_3)_2$ ). The powder was collected and dried in vacuo {yield 92% based on **[1]** ( $[\text{1}](\text{NO}_3)_2$ )}. ESI-MS (in  $\text{CH}_3\text{CN}$ ):  $m/z$  285.1 **[3]**<sup>2+</sup>; relative intensity (*I*) = 100% in the range of  $m/z$  100–2000.  $^1\text{H}$  NMR (300 MHz, in  $\text{D}_2\text{O}$ , reference to TSP, pD 6.6, 25 °C):  $\delta$  2.15 {s, 18H,  $\text{C}_6(\text{CH}_3)_6$ }, 2.62 (s, 6H, N– $\text{CH}_3$ ), 1.66–1.94, 2.10–2.32, 2.48–2.82, 3.14–3.24 (m, 14H, – $\text{CH}_2$ –). FT-IR ( $\text{cm}^{-1}$ , KBr disk): 1988 (C≡O). XPS (eV): 854.2 (Ni 2p<sub>3/2</sub> region), 280.7 (Ru 3d<sub>5/2</sub> region).

$[\text{Ni}^{\text{II}}\text{LRu}^{\text{II}}(\text{CO})(\eta^6\text{-C}_6\text{Me}_6)](\text{OTf})_2$  **[3]** ( $[\text{3}](\text{OTf})_2$ ). An aqueous solution (1.0 mL) of NaOTf (172 mg 1.0 mmol) was added to an aqueous solution of **[3]** ( $[\text{3}](\text{NO}_3)_2$ ) (306 mg, 0.44 mmol) at 25 °C. After a brown oil was filtered out, NaOTf (1.72 g 10 mmol) was added to the resulting solution to give a red crystal of **[3]** ( $[\text{3}](\text{OTf})_2$ ), which was collected and dried in vacuo {yield 24% based on **[3]** ( $[\text{3}](\text{NO}_3)_2$ )}. ESI-MS (in  $\text{H}_2\text{O}$ ):  $m/z$  271.0 **[3]**–CO<sup>+</sup>; *I* = 100% in the range of  $m/z$  100–2000, 719.0 **[3]** + OTf<sup>+</sup>; *I* = 57% in the range of  $m/z$  100–2000.  $^1\text{H}$  NMR (300 MHz, in  $\text{D}_2\text{O}$ , reference to TSP, pD 6.6, 25 °C):  $\delta$  2.15 {s, 18H,  $\text{C}_6(\text{CH}_3)_6$ }, 2.62 (s, 6H, N– $\text{CH}_3$ ), 1.64–1.84, 2.04–2.42, 2.53–2.78, 3.10–3.18 (m, 14H, – $\text{CH}_2$ –).  $^{13}\text{C}$  NMR (300 MHz, in  $\text{D}_2\text{O}$ , reference to 1,4-dioxane, pD 6.6, 25 °C): 198.78, 112.82, 72.16, 61.00, 43.30, 29.72, 24.04, 16.60. FT-IR ( $\text{cm}^{-1}$ , KBr disk): 1989 (C≡O). Anal. Calcd for **[3]** ( $[\text{3}](\text{OTf})_2$ ):  $\text{C}_{24}\text{H}_{38}\text{F}_6\text{N}_2\text{NiO}_7\text{RuS}_4\cdot\text{H}_2\text{O}$ : C, 32.51; H, 4.55; N, 3.16. Found: C, 32.62; H, 4.46; N, 3.18.

**Reaction of 1 with a Gas Mixture of CO (0.05 MPa) and  $\text{H}_2$  (0.05 MPa) in Water.** A gas mixture of CO (0.05 MPa) and  $\text{H}_2$  (0.05 MPa) was bubbled through an aqueous solution of **[1]** ( $[\text{1}](\text{NO}_3)_2$ ) (0.10 mM) at 20 °C to quantitatively afford the CO complex **3**, which was confirmed by UV–vis spectroscopy and ESI-MS.

**Kinetic Measurement of the Reaction of 1 with CO.** The reaction rate of **1** with CO in CO-saturated methanol at –70 °C under

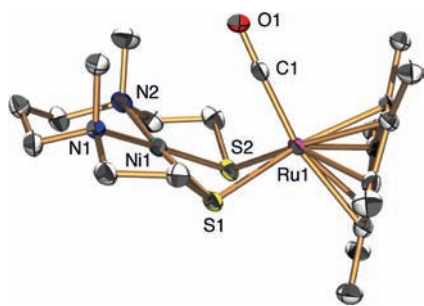


**Figure 3.** ORTEP drawing of  $[3](\text{OTf})_2$  with 50% probability. Counteranions ( $\text{OTf}$ ) and solvents ( $\text{H}_2\text{O}$ ) were omitted for clarity. Selected interatomic distances ( $\text{\AA}$ ) and angles ( $^\circ$ ):  $\text{Ni1}\cdots\text{Ru1} = 3.125(1)$ ,  $\text{Ru1}-\text{C1} = 1.883(4)$ ,  $\text{Ru1}-\text{S1} = 2.393(1)$ ,  $\text{Ru1}-\text{S2} = 2.388(1)$ ,  $\text{Ni1}-\text{S1} = 2.164(1)$ ,  $\text{Ni1}-\text{S2} = 2.168(1)$ ,  $\text{Ni1}-\text{N1} = 1.985(4)$ ,  $\text{Ni1}-\text{N2} = 1.981(4)$ ,  $\text{C1}-\text{O1} = 1.135(5)$ ,  $\text{Ni1}-\text{S1}-\text{Ru1} = 86.42(4)$ ,  $\text{Ni1}-\text{S2}-\text{Ru1} = 86.47(4)$ ,  $\text{Ru1}-\text{C1}-\text{O1} = 177.8(3)$ .

CO was followed by UV-vis spectral change (299 nm) measured with an Otsuka Electronics photodiode array spectrometer MCPD-2000. Methanol (9.90 mL) in a 3-neck flask (25 mL) at  $-70^\circ\text{C}$  was bubbled through CO gas for 30 min to give a CO-saturated methanol solution. Then to the resulting solution was added a methanol solution of **1** (7.8 mM, 0.10 mL). The final concentration of **1** was 0.078 mM. The pseudo-first-order rate constant  $k_{\text{obs}}$  ( $k_{\text{obs}} = 1.5 \times 10^{-3} \text{ s}^{-1}$ ) was determined by a least-squares curve fit.

**X-ray Crystallographic Analysis.** Measurements were made on a Rigaku/MSM Mercury CCD diffractometer with graphite monochromated Mo  $K\alpha$  radiation ( $\lambda = 0.7107 \text{ \AA}$ ). All calculations were performed using the teXsan crystallographic software package of Molecular Structure Corp. Crystallographic data for  $[3](\text{OTf})_2$  have been deposited with the Cambridge Crystallographic Data Center as Supplementary Publication No. CCDC-758805. Copies of the data can be obtained free of charge on application to CCDC, 12 Union Road, Cambridge CB2 1EZ, U.K.

## RESULTS AND DISCUSSION

**Synthesis and Structure of the CO Complex **3**.** The aqua complex of  $[1](\text{NO}_3)_2$  rapidly reacts with CO in water to give a dark red solution of the CO complex  $[3](\text{NO}_3)_2$ . The solid state structure of  $[3]^{2+}$  was determined by X-ray analysis from a red crystal of  $[3](\text{OTf})_2$ , prepared by anion exchange of  $[3](\text{NO}_3)_2$  with NaOTf in water (Figure 3). The CO ligand was coordinated to the Ru center with a  $\text{Ru1}-\text{C1}$  length of 1.883(4)  $\text{\AA}$  and a  $\text{Ru1}-\text{C1}-\text{O1}$  angle of  $177.8(3)^\circ$ . The C–O bond length {1.135(5)  $\text{\AA}$ } is almost comparable to that of a free CO (1.128  $\text{\AA}$ ).<sup>16</sup> The structure of **3** contains a  $\text{Ni}_2\text{Ru}$  butterfly core, in which the Ni atom and the Ru atom are joined by a pair of bidentate thiolato ligands. The Ni atom adopts a square planar geometry with the tetradentate ligand L, whereas the Ru atom adopts distorted octahedral coordination which is surrounded by one CO, one hexamethylbenzene ligand, and one metalloligand  $[\text{Ni}^{\text{II}}\text{L}]$ . The  $\text{Ni1}-\text{S1}-\text{Ru1}$  and  $\text{Ni1}-\text{S2}-\text{Ru1}$  angles are  $86.42(4)^\circ$  and  $86.47(4)^\circ$ , respectively. The  $\text{Ni1}\cdots\text{Ru1}$  distance {3.125(1)  $\text{\AA}$ } of **3** is comparable to that {3.1611(6)  $\text{\AA}$ } of **1**.<sup>7</sup> A significant difference from **1** is the direction of methyl groups of the tetradentate ligand L coordinated to  $\text{Ni}^{\text{II}}$  center.

An important difference between the structure of  $[3]^{2+}$  and that of the Ni–CO form (Ni–SCO) produced by Higuchi et al. is shown in the site of CO binding. Our crystal structure shows

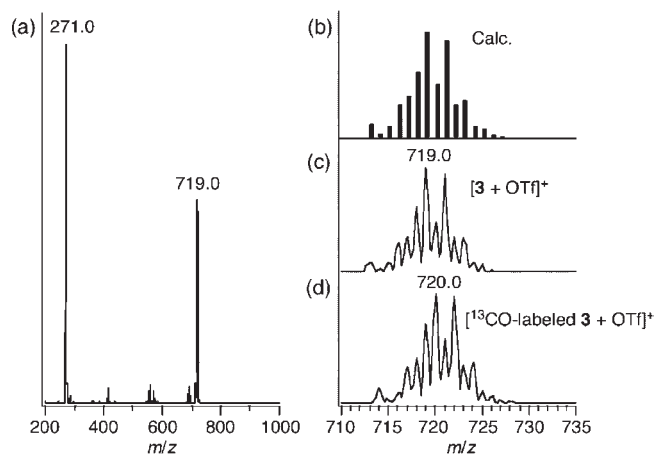


**Figure 4.** (a) Positive-ion ESI mass spectrum of  $[3](\text{OTf})_2$  in water. The signal at  $m/z$  271.0 corresponds to  $[3 - \text{CO}]^{2+}$  ( $I = 100\%$  in the range of  $m/z$  100–2000) and  $m/z$  719.0 corresponds to  $[3 + \text{OTf}]^+$  ( $I = 57\%$  in the range of  $m/z$  100–2000). (b) Calculated isotopic distribution for  $[3 + \text{OTf}]^+$ . (c) The signal at  $m/z$  719.0 was for  $[3 + \text{OTf}]^+$ . (d) Positive-ion ESI mass spectrum of  $[^{13}\text{C}]\text{-labeled } [3 + \text{OTf}]^+$  in water.

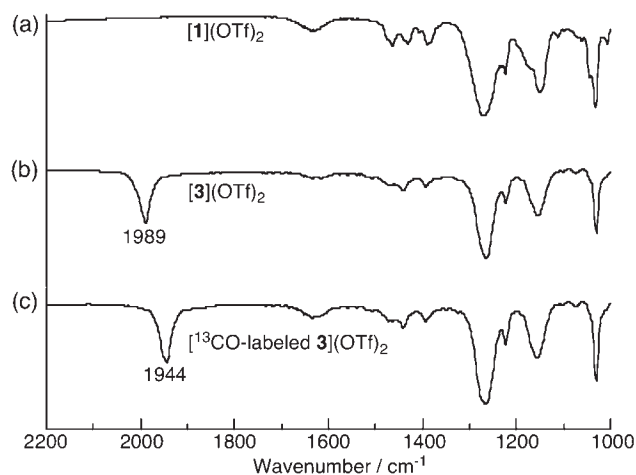


**Figure 5.** IR spectra as KBr disks of (a)  $[1](\text{OTf})_2$ , (b)  $[3](\text{OTf})_2$ , and (c)  $[^{13}\text{C}]\text{-labeled } [3](\text{OTf})_2$ .

that the CO ligand is coordinated to the Ru center, equivalent to the Fe center of  $[\text{NiFe}]_2\text{H}_2\text{ase}$ , whereas their structure shows CO coordinated to the Ni center. That CO would prefer coordination to  $\text{Ru}^{\text{II}}$ , rather than taking an axial position on the Ni, is predictable using the principles of coordination chemistry. Higuchi's structure, showing CO coordinated to a Ni center (Ni–SCO), therefore provides further evidence that the  $\text{Fe}^{\text{II}}$  position must already be occupied. Since Higuchi and co-workers used crystals of the hydride complex as starting material,<sup>3c</sup> we are convinced that, in their case, the hydrido ligand remains in place in its bridging position between the two metal centers (Ni–HCO).

Figure 4 shows a positive-ion ESI mass spectrum of  $[3](\text{OTf})_2$  in water. The prominent signal at  $m/z$  719.0 ( $I = 57\%$  in the range of  $m/z$  100–2000) has a characteristic isotopic distribution that matches well with the calculated isotopic distribution for  $[3 + \text{OTf}]^+$ . To establish the origin of the CO ligand of **3**, synthesis of  $^{13}\text{C}$ -labeled **3** by reaction of **1** with  $^{13}\text{C}$  in water for 1 h at  $25^\circ\text{C}$

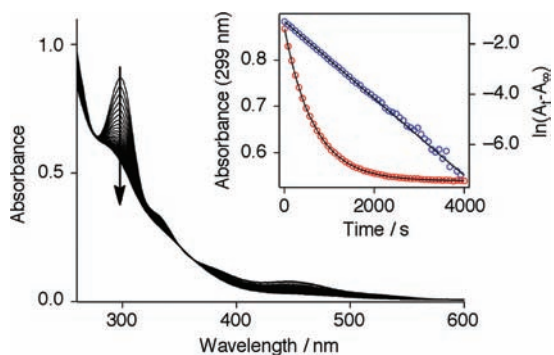


**Figure 6.** UV-vis spectral change for the reaction of **1** (0.078 mM) with CO in CO-saturated methanol at  $-70\text{ }^{\circ}\text{C}$  (time interval 80 s). (Inset) Time profile of the absorbance at 299 nm (curve) and the pseudo-first-order plot (linear plot).

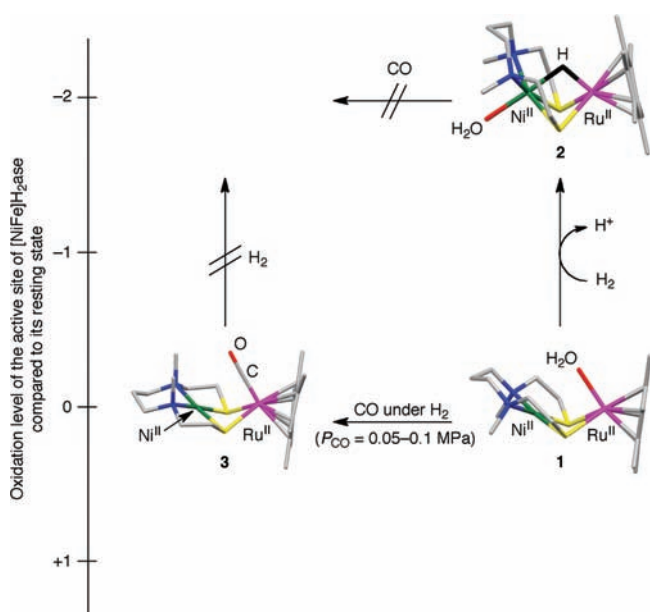


**Figure 7.** Schematic representation of the  $[\text{NiFe}]\text{H}_2\text{ase}$  model complexes **1**,<sup>7a</sup> **2**,<sup>7a</sup> and **3** whose structures were determined by X-ray analysis.  $P_{\text{CO}}$  represents the partial pressure of CO in the CO/ $\text{H}_2$  system, where the total pressure is 0.1 MPa.

was carried out. ESI-MS results show that the signal at  $m/z$  719.0 shifts to  $m/z$  720.0. This indicates that the  $^{13}\text{C}$  atom is incorporated in **3**.

Figure 5 shows the IR spectra of  $[\mathbf{1}](\text{OTf})_2$ ,  $[\mathbf{3}](\text{OTf})_2$ , and  $[\mathbf{1}^{13}\text{CO-labeled } \mathbf{3}](\text{OTf})_2$ , recorded using KBr disks. The vibration mode of the CO ligand was observed at  $1989\text{ cm}^{-1}$  characteristic of the terminal CO group<sup>16</sup> and in the case of  $^{13}\text{CO}$  was shifted to  $1944\text{ cm}^{-1}$ . The shift value ( $45\text{ cm}^{-1}$ ) agrees well with that expected by a Hooke's law calculation for a pure CO stretching mode.<sup>17</sup> This shift in peak position for the isotopomer demonstrates that the CO ligand originates from the CO feed and is not from  $\text{H}_2$ -reduced  $\text{CO}_2$  in the solvent. A free CO molecule has a stretching frequency of  $2143\text{ cm}^{-1}$ .<sup>16</sup> The frequency of CO coordinated to the  $\text{Ru}^{\text{II}}$  center in **3** is lower than that of free CO, which is consistent with back-donation of electron density from the  $t_{2g}$  orbital of  $\text{Ru}^{\text{II}}$  to the  $\pi^*$ -antibonding orbital of CO.

XPS of  $[\mathbf{3}](\text{NO}_3)_2$  shows that the binding energies of Ni  $2p_{3/2}$  and Ru  $3d_{5/2}$  are 854.2 and 280.7 eV, which correspond to Ni(II) and Ru(II), respectively.<sup>14</sup> The values of the binding energies of Ni  $2p_{3/2}$  and Ru  $3d_{5/2}$  in **3** are comparable to those in  $[\mathbf{1}](\text{NO}_3)_2$  (Ni  $2p_{3/2}$  853.9 eV, Ru  $3d_{5/2}$  280.5 eV).<sup>7b</sup>

Analysis of kinetic data obtained by monitoring a decrease of the absorbance band at 299 nm of **1** revealed that reaction of **1** with CO in CO-saturated methanol<sup>18</sup> at  $-70\text{ }^{\circ}\text{C}$  followed pseudo-first-order kinetics with respect to **1** (Figure 6). The rate constant ( $k_{\text{obs}} = 1.5 \times 10^{-3}\text{ s}^{-1}$ ) of the reaction was determined by a least-squares curve fit.

**Effect of CO Ligand for  $\text{H}_2$  Activation in Water.** The CO-coordinated complex, **3**, was unable to activate  $\text{H}_2$ , which was equivalent to complete inhibition of compound **1** by CO (Figure 7). The reaction was conducted over a pH range of 4.0–9.0 and monitored by ESI-MS. No hydride or  $\text{H}_2$  products were observed, demonstrating similar behavior to that expected for CO-inhibited  $[\text{NiFe}]\text{H}_2\text{ase}$ .<sup>1,3c,12</sup>

We also conducted competition experiments using CO/ $\text{H}_2$  mixture. In a simple experiment, free complex **1** was exposed to a 1:1 mixture of CO and  $\text{H}_2$  (0.05 MPa of CO and 0.05 MPa of  $\text{H}_2$ ). This resulted in a 100% yield of CO-coordinated **3** but no  $\text{H}^-$ -coordinated **2**. CO was clearly able to outcompete  $\text{H}_2$  for the Ru site and, since the Ru site in our complex **3** is a direct analogue for the Fe site in Fe–CO of  $[\text{NiFe}]\text{H}_2\text{ase}$  (Figure 2), it is therefore most likely that the same process occurs in the natural enzyme, even after accounting for the greater affinity of CO for  $\text{Ru}^{\text{II}}$  over  $\text{Fe}^{\text{II}}$ .

**Reactivity of the Hydride Complex **2** with CO in Water.** The reactivity of CO with the hydride complex **2** was also investigated. Once **2** was formed by reaction of **1** with  $\text{H}_2$ , reactions with CO were not observed. Clearly, CO is not able to displace either the  $\text{H}^-$  ligand or the Ni-coordinated axial aqua ligand of **2**. Presumably, this exchange would be unfavorable as six-coordinate Ni–CO compounds are very unusual and **2**, therefore, can be considered as having no vacant binding sites for CO.

This observation explains why the CO ligand in the Higuchi complex is found on the Ni center (Ni–SCO). In this case, the Fe site is blocked by the preformed hydride but the planar Ni site is still vacant (Ni–C). Ni coordination is not observed in **2** as it does not have a vacant planar site.

We suggest that Higuchi's crystal structure is actually that of a hydride complex (Ni–HCO). Our experimental results demonstrate that (i) CO preferentially binds to the Fe-equivalent Ru center rather than an axial position on the Ni center, (ii)  $\text{H}_2$  cannot displace CO from the Ru center, and (iii) CO is unable to displace  $\text{H}^-$  from the Ru center. These conclusions may be drawn from not only this work but also further model and enzymatic studies.<sup>1,3c,12,19</sup>

By combining the following experimental observations and chemical reasoning, we propose a modified mechanism for CO inhibition. Using a  $[\text{NiFe}]\text{H}_2\text{ase}$  mimic, we demonstrated that CO prefers to bind to the Fe-equivalent Ru center. We have also shown that (i)  $\text{H}_2$  cannot displace CO, which accounts for the inhibition, and (ii) CO cannot displace  $\text{H}^-$ , accounting for Higuchi's crystal structure bearing a Ni-coordinated CO. In short, CO inhibits  $[\text{NiFe}]\text{H}_2\text{ase}$  by preferentially binding to the Fe center.

## CONCLUSIONS

We presented experimental evidence, based on a  $[\text{NiFe}]\text{H}_2\text{ase}$  mimic, to support a modified mechanism for CO inhibition. We

propose that, rather than the Ni center, CO binds to the Fe center of [NiFe]<sub>2</sub>H<sub>2</sub>ase. We believe this revision will lead to a greater understanding of this potentially important enzyme. These studies continue to confirm the reciprocal benefits of convergent biological and chemical investigations. We are keen to develop this theme, especially in the form of the emerging field of bioinspired catalysis.

## ■ ASSOCIATED CONTENT

**S** Supporting Information. This material is available free of charge via the Internet at <http://pubs.acs.org>.

## ■ AUTHOR INFORMATION

### Corresponding Author

\*Phone +81-92-802-2818. Fax: +81-92-802-2823. E-mail: [ogotcm@mail.cstm.kyushu-u.ac.jp](mailto:ogotcm@mail.cstm.kyushu-u.ac.jp).

## ■ ACKNOWLEDGMENT

We thank Professor Kiyoshi Isobe for valuable discussions. This work was supported by the World Premier International Research Center Initiative (WPI Program), grants-in-aid 18065017 (Chemistry of Concerto Catalysis), 19205009, and 23655053, the Global COE Program, "Science for Future Molecular Systems" from the Ministry of Education, Culture, Sports, Science and Technology (MEXT), Japan, and the Basic Research Programs CREST Type "Development of the Foundation for Nano-Interface Technology" from JST, Japan.

## ■ REFERENCES

- (1) (a) Special issue on hydrogenases: *Eur. J. Inorg. Chem.* **2011**, 915–1171. (b) Special issue on renewable energy: *Chem. Soc. Rev.* **2009**, 38, 1–300. (c) Special issue on hydrogen: *Chem. Soc. Rev.* **2007**, 107, 3900–4435. (d) Special issue on hydrogenases: *Coord. Chem. Rev.* **2005**, 249, 1517–1690. (e) Tard, C.; Pickett, C. J. *Chem. Rev.* **2009**, 109, 2245–2274. (f) Ogata, H.; Lubitz, W.; Higuchi, Y. *Dalton Trans.* **2009**, 7577–7587. (g) Stein, M.; Lubitz, W. *J. Inorg. Biochem.* **2004**, 98, 862–877.
- (2) (a) Volbeda, A.; Charon, M.-H.; Piras, C.; Hatchikian, E. C.; Frey, M.; Fontecilla-Camps, J. C. *Nature* **1995**, 373, 580–587. (b) Volbeda, A.; Garcin, E.; Piras, C.; de Lacy, A. L.; Fernandez, V. M.; Hatchikian, E. C.; Frey, M.; Fontecilla-Camps, J. C. *J. Am. Chem. Soc.* **1996**, 118, 12989–12996.
- (3) (a) Higuchi, Y.; Yagi, T.; Yasuoka, N. *Structure* **1997**, 5, 1671–1680. (b) Higuchi, Y.; Ogata, H.; Miki, K.; Yasuoka, N.; Yagi, T. *Structure* **1999**, 7, 549–556. (c) Ogata, H.; Mizoguchi, Y.; Mizuno, N.; Miki, K.; Adachi, S.; Yasuoka, N.; Yagi, T.; Yamauchi, O.; Hirota, S.; Higuchi, Y. *J. Am. Chem. Soc.* **2002**, 124, 11628–11635. (d) Ogata, H.; Hirota, S.; Nakahara, A.; Komori, H.; Shibata, N.; Kato, T.; Kano, K.; Higuchi, Y. *Structure* **2005**, 13, 1635–1642. (e) van Gestel, M.; Stein, M.; Brecht, M.; Schröder, O.; Lendzian, F.; Bittl, R.; Ogata, H.; Higuchi, Y.; Lubitz, W. *J. Biol. Inorg. Chem.* **2006**, 11, 41–51.
- (4) (a) Peters, J. W.; Lanzilotta, W. N.; Lemon, B. J.; Seefeldt, L. C. *Science* **1998**, 282, 1853–1858. (b) Nicolet, Y.; Piras, C.; Legrand, P.; Hatchikian, E. C.; Fontecilla-Camps, J. C. *Structure* **1999**, 7, 13–23.
- (5) Shima, S.; Pilak, O.; Vogt, S.; Schick, M.; Stagni, M. S.; Meyer-Klaucke, W.; Warkentin, E.; Thauer, R. K.; Ermler, U. *Science* **2008**, 321, 572–575.
- (6) (a) Special issue on the hydrogen economy. *Science* **2004**, 305, 957–976. (b) Crabtree, G. W.; Dresselhaus, M. S. *MRS Bull.* **2008**, 33, 421–428. (c) Jacobson, M. Z.; Colella, W. G.; Golden, D. M. *Science* **2005**, 308, 1901–1905. (d) Cammack, R. *Nature* **1999**, 397, 214–215. (e) Adams, M. W. W.; Stiefel, E. I. *Science* **1998**, 282, 1842–1843. (f) Adams, M. W. W. *Biochim. Biophys. Acta* **1990**, 1020, 115–145.
- (7) (a) Ogo, S.; Kabe, R.; Uehara, K.; Kure, B.; Nishimura, T.; Menon, S. C.; Harada, R.; Fukuzumi, S.; Higuchi, Y.; Ohhara, T.; Tamada, T.; Kuroki, R. *Science* **2007**, 316, 585–587. (b) Ogo, S. *Chem. Commun.* **2009**, 3317–3325.
- (8) (a) Yagi, T.; Tsuda, M.; Inokuchi, H. *J. Biochem.* **1973**, 73, 1069–1081. (b) Fauque, G. D.; Berlier, Y. M.; Czechowski, M. H.; Dimon, B.; Lespinat, P. A.; LeGall, J. *J. Ind. Microbiol.* **1987**, 2, 15–23. (c) Zorin, N. A.; Dimon, B.; Gagnon, J.; Gaillard, J.; Carrier, P.; Vignais, P. M. *Eur. J. Biochem.* **1996**, 241, 675–681. (d) Bernhard, M.; Buhrke, T.; Bleijlevens, B.; de Lacey, A. L.; Fernandez, V. M.; Albracht, S. P. J.; Friedrich, B. *J. Biol. Chem.* **2001**, 276, 15592–15597. (e) Vignais, P. M.; Cournac, L.; Hatchikian, E. C.; Elsen, S.; Serebryakova, L.; Zorin, N.; Dimon, B. *Int. J. Hydrogen Energy* **2002**, 27, 1441–1448. (f) Vignais, P. M.; Dimon, B.; Zorin, N. A.; Tomiyama, M.; Colbeau, A. *J. Bacteriol.* **2000**, 182, 5997–6004. (g) Cournac, L.; Guedeny, G.; Peltier, G.; Vignais, P. M. *J. Bacteriol.* **2004**, 186, 1737–1746. (h) Vogt, S.; Lyon, E. J.; Shima, S.; Thauer, R. K. *J. Biol. Inorg. Chem.* **2008**, 13, 97–106.
- (9) Teixeira, M.; Fauque, G.; Moura, I.; Lespinat, P. A.; Berlier, Y.; Prickril, B.; Peck, H. D., Jr.; Xavier, A. V.; LeGall, J.; Moura, J. J. G. *Eur. J. Biochem.* **1987**, 167, 47–58.
- (10) Hatchikian, E. C.; Forget, N.; Fernandez, V. M.; Williams, R.; Cammack, R. *Eur. J. Biochem.* **1992**, 209, 357–365.
- (11) Thauer, R. K.; Klein, A. R.; Hartmann, G. C. *Chem. Rev.* **1996**, 96, 3031–3042.
- (12) (a) Yagi, T.; Kimura, K.; Daidoji, H.; Sakai, F.; Tamura, S.; Inokuchi, H. *J. Biochem.* **1976**, 79, 661–671. (b) van der Zwaan, J. W.; Coremans, J. M. C. C.; Bouwens, E. C. M.; Albracht, S. P. J. *Biochim. Biophys. Acta* **1990**, 1041, 101–110. (c) Bagley, K. A.; van Garderen, C. J.; Chen, M.; Duin, E. C.; Albracht, S. P. J.; Woodruff, W. H. *Biochemistry* **1994**, 33, 9229–9236. (d) George, S. J.; Kurkin, S.; Thorneley, R. N. F.; Albracht, S. P. J. *Biochemistry* **2004**, 43, 6808–6819. (e) Pandelia, M.-E.; Ogata, H.; Currell, L. J.; Flores, M.; Lubitz, W. *Biochim. Biophys. Acta* **2010**, 1797, 304–313.
- (13) Ogo, S. *Dalton Trans.* **2010**, 39, 2963.
- (14) Moulder, J. F.; Stickle, W. F.; Sobol, P. E.; Bomben, K. D. *Handbook of X-ray Photoelectron Spectroscopy*; Physical Electronics: Eden Prairie, MN, 1995.
- (15) (a) Glasoe, P. K.; Long, F. A. *J. Phys. Chem.* **1960**, 64, 188–190. (b) Mikkelsen, K.; Nielsen, S. O. *J. Phys. Chem.* **1960**, 64, 632–637.
- (16) (a) Cotton, F. A.; Wilkinson, G.; Murillo, C. A.; Bochmann, M. *Advanced Inorganic Chemistry*, 6th ed.; John Wiley & Sons: New York, 1999; pp 636–639. (b) Reynolds, M. A.; Rauchfuss, T. B.; Wilson, S. R. *Organometallics* **2003**, 22, 1619–1625. (c) Oudart, Y.; Artero, V.; Pécaut, J.; Lebrun, C.; Fontecave, M. *Eur. J. Inorg. Chem.* **2007**, 2613–2626.
- (17) Nakamoto, K. *Infrared and Raman Spectra of Inorganic and Coordination Compounds*, 5th ed.; Wiley: New York, 1997 and references therein.
- (18) Methanol was used as a solvent for the kinetic measurement at –70 °C because reaction of **1** with CO in CO-saturated water at 5 °C was completed within 1 s.
- (19) (a) Zhu, W.; Marr, A. C.; Wang, Q.; Neese, F.; Spencer, D. J. E.; Blake, A. J.; Cooke, P. A.; Wilson, C.; Schröder, M. *Proc. Natl. Acad. Sci. U.S.A.* **2005**, 102, 18280–18285. (b) Hsieh, C.-H.; Chupik, R. B.; Brothers, S. M.; Hall, M. B.; Darensbourg, M. Y. *Dalton Trans.* **2011**, 40, 6047–6053. (c) Ohki, Y.; Yasumura, K.; Ando, M.; Shimokata, S.; Tatsumi, K. *Proc. Natl. Acad. Sci. U.S.A.* **2010**, 107, 3994–3997.